

# Acupuncture Ameliorates Alzheimer's-Like Cognitive Impairment and Pathological Changes via Regulating the Intestinal Fungal Community in APP/PS1 Mice

Xin Hao<sup>1,\*</sup>, Ning Ding<sup>2,\*</sup>, Yue Zhang<sup>3</sup>, Meng Wu<sup>1</sup>, Yilin Tao<sup>1</sup>, Zhigang Li<sup>1</sup>

<sup>1</sup>School of Acupuncture, Moxibustion and Tuina, Beijing University of Chinese Medicine, Beijing, 100029, People's Republic of China; <sup>2</sup>Guang'anmen Hospital, China Academy of Chinese Medical Sciences, Beijing, 100053, People's Republic of China; <sup>3</sup>Guangzhou University of Chinese Medicine Meizhou Hospital (Meizhou Hospital of Chinese Medicine), Guangzhou, 514000, People's Republic of China

\*These authors contributed equally to this work

Correspondence: Ning Ding, Guang'anmen Hospital, China Academy of Chinese Medical Sciences, Beijing, 100053, People's Republic of China, Email [beijingdingning@163.com](mailto:beijingdingning@163.com); Zhigang Li, School of Acupuncture, Moxibustion and Tuina, Beijing University of Chinese Medicine, Beijing, 100029, People's Republic of China, Email [lizhigang620@126.com](mailto:lizhigang620@126.com)

**Background:** The disorder of the intestinal fungal community is closely associated with Alzheimer's disease (AD). Gut fungal dysbiosis exacerbates  $\beta$ -amyloid ( $A\beta$ ) plaque burden through the brain-gut axis, thereby promoting the progression of AD. Previous research has demonstrated that acupuncture can ameliorate AD symptoms by modulating the gut bacterial community. However, the potential regulatory effects of acupuncture on the fungal microbiota have been largely overlooked.

**Methods:** APP/PS1 mice were used as AD animal model and randomly divided into the AD model (AD) group, the acupuncture (Ac) group, and the probiotics (Pr) group. Mice in the Ac group received acupuncture treatment. In the Pr group, mice were treated with probiotics. Morris water maze, ITS sequencing, immunofluorescence (IF) staining, enzyme-linked immunosorbent assay (ELISA), Hematoxylin and eosin analysis, and Nissl staining were employed to validate our hypothesis.

**Results:** Acupuncture and probiotics significantly improved the behavioral performance of APP/PS1 mice, reduced the level of  $A\beta$  in the brain, and alleviated neuronal damage. Moreover, acupuncture improved the Sobs, Chao and Ace indices, decreased the abundance of *Ascomycota*, *Aspergillaceae*, *Trichocomaceae*, *Candida*, and *unclassified-penicillium*, while simultaneously increasing the abundance of *Basidiomycota*, which differed from the fungal regulation observed with probiotics.

**Conclusion:** Acupuncture may improve the cognitive impairment of APP/PS1 mice, reduce  $A\beta$  plaque burden in the brain, protect neurons, and mitigate intestinal fungi dysbiosis. The beneficial effects of acupuncture on  $A\beta$  deposition and cognitive function in APP/PS1 mice may be achieved by regulating the intestinal fungal community.

**Keywords:** Alzheimer's disease, acupuncture, intestinal fungal community,  $\beta$ -amyloid, probiotics

## Introduction

Alzheimer's disease (AD) is a neurodegenerative disease characterized by an insidious onset and progressive development. The primary clinical manifestations include memory impairment and executive dysfunction, often accompanied by alterations in personality and behavior. According to statistics,<sup>1</sup> the number of AD patients has reached 55 million globally and is expected to exceed 135 million by 2050, imposing a heavy burden on families and society. The pathogenesis of AD is a complex process with multifactorial influences, in which the overproduction of  $\beta$ -amyloid ( $A\beta$ ) and its deposition in the brain are considered to be a central link.<sup>2</sup> The senile plaques resulting from the abnormal deposition of  $A\beta$  and the neurofibrillary tangles formed by the hyperphosphorylation of tau protein are not only pathological products of AD but also its main pathological features. However, pharmacological interventions aimed at

removing A $\beta$  plaques and tau proteins have so far been unsuccessful. Therefore, it is imperative to further investigate the pathogenesis of AD and identify new effective therapeutic targets.

In addition to central mechanisms, the gut microbiota has been recognized as a crucial factor in the development of neuropathological changes associated with AD.<sup>3–5</sup> The gut microbiota encompasses a vast and diverse community of microorganisms, including bacteria, archaea, fungi, viruses, prokaryotes, etc. This intricate ecosystem is essential for maintaining host homeostasis.<sup>6</sup> Historically, research on gut microbiota has predominantly focused on bacteria, due to their dominant role in the human intestine. Alterations in the composition and diversity of intestinal bacteria have been reported to correlate with AD pathology.<sup>7</sup> Despite constituting a minor fraction of the gut microbiota, the influence of intestinal fungi on the organism cannot be overlooked.<sup>8</sup> In recent years, the relationship between the intestinal fungal community and the central nervous system has garnered increasing attention.<sup>9,10</sup> Multiple studies have demonstrated that significant alterations in the fungal microbiota are associated with various neurological disorders, such as Parkinson's disease, depression, bipolar disorder and AD.<sup>11–13</sup> Changes in the structure of the intestinal fungi are closely correlated with the levels of pathological biomarkers of AD (A $\beta$ , tau, etc).<sup>14</sup> A recent study revealed that dysbiosis of intestinal fungi exacerbates A $\beta$  deposition and neuroinflammation via the brain-gut axis.<sup>15</sup> Modulating the homeostasis of the fungal microbiota can inhibit microglia-induced neuroinflammation, reduce A $\beta$  plaque burden and tau pathology, and ultimately ameliorate the cognitive deficits characteristic of AD.<sup>16</sup> Therefore, Intestinal fungi may represent a potential target for alleviating pathological damage and enhancing cognitive function in AD.

As an important component of traditional Chinese medicine, acupuncture has been extensively utilized in clinical practice due to its low cost, minimal side effects, and prominent therapeutic efficacy. Numerous researches have demonstrated that acupuncture could improve the learning and memory ability of AD model animals through various mechanisms, including the elevation of cerebral blood flow in the hippocampus and prefrontal cortex,<sup>17</sup> enhancement of cerebral glucose metabolism,<sup>18</sup> inhibition of glial cell activation,<sup>19</sup> regulation of A $\beta$  production and clearance,<sup>20,21</sup> and prevention of neuronal apoptosis.<sup>22</sup> Our previous studies have confirmed that acupuncture can rectify intestinal flora disorder in APP/PS1 mice, mitigate the intestinal inflammatory response, and protect both the intestinal mucosal barrier and the blood-brain barrier.<sup>23,24</sup> Additionally, our findings indicated that intestinal flora may serve as a critical target for acupuncture in inhibiting neuroinflammation and enhancing cognitive function. However, these studies have predominantly concentrated on the modulation of gut bacterial diversity and composition by acupuncture, while the effects on fungal microbiota have been largely overlooked. Given that A $\beta$  deposition in the hippocampus is a critical pathological factor in the progression of AD and is intricately linked with intestinal fungi dysbiosis, it is imperative to elucidate whether acupuncture can balance intestinal fungi, reduce cerebral A $\beta$  accumulation, and improve cognitive function in AD. In view of this, we investigated the effects of acupuncture on cognitive ability, intestinal fungi, and A $\beta$  levels in the hippocampus of APP/PS1 mice. Our study aimed to elucidate the mechanisms through which acupuncture ameliorates cognitive impairment in AD, particularly from the perspective of intestinal fungi. The findings of this research will provide more evidence for clarifying the intestinal mechanisms of acupuncture in the treatment of AD.

## Material and Methods

### Experimental Animals

APPswe/PS1 $\Delta$ E9 (APP/PS1) transgenic animals (male, 6-month old, 28–32 g) with C57BL/6 background and their corresponding wild-type C57BL/6 littermates (male, 6-month old, 28–32 g) were obtained from Cavens Biogleg Model Animal Research Co. Ltd. (Suzhou, China). All mice were maintained in the Experimental Animal Center of the Beijing University of Chinese Medicine, which was SPF conditions, with a temperature of  $24 \pm 2^\circ\text{C}$ , a 12-h dark/light cycle, access to sterile drinking water and a standard pellet diet. The animals were acclimatized to the environment for 7 days before experimentation, and all experimental procedures conformed to the National Institutes of Health Guidelines for the Care and Use of Laboratory Animals, with the approval of the Beijing University of Chinese Medicine, Beijing, China (ID: bucm-4-2,021,102,701-4032).

## Animal Grouping and Intervention

Wild-type C57BL/6 mice served as controls (WT group,  $n = 12$ ). APP/PS1 mice were separated randomly into three groups ( $n = 12$  per group): the AD model (AD) group, the acupuncture (Ac) group, and the probiotics (Pr) group.

In the Ac group, the mice were placed and immobilized in self-made conical mouse bags. Baihui (GV20), Yintang (GV29) and Zusanli (ST36) were selected for acupuncture intervention. According to our previous research,<sup>25,26</sup> the disposable sterile acupuncture needles (diameter, 0.25 mm; length, 13 mm; Zhongyan Taihe, Beijing, China) were inserted obliquely upward at an angle of  $15^\circ$  to a depth of 2–3 mm at GV20 and GV29. At ST36, the needle was inserted perpendicularly to a depth of 4 mm. During the needling process, the needle was twisted bidirectionally within  $90^\circ$  for 15 seconds at intervals of 5 minutes. This acupuncture intervention lasted for 4 weeks, once a day for 20 minutes. For the Pr group, probiotics ( $8.7 \times 10^8$  CFU/g/d, Zhongke Yikang Biotechnology Company, Beijing, China) were administered by gavage once a day for 4 weeks.<sup>27</sup> Mice in the WT and AD groups received no treatment. During acupuncture, mice in the WT, AD and Pr groups were immobilized for 20 minutes in the same manner as those in the Ac group.

## Morris Water Maze Test

On day 30, ten mice were randomly selected from each group for Morris water maze (MWM) test, and related interventions were performed simultaneously. The MWM device consists of a 90 cm diameter circular pool, which is divided into four quadrants. In the hidden platform trial, the platform is located 1 cm below the water surface in the center of the southwest (SW) quadrant. Following the established experimental protocol,<sup>28</sup> each mouse was allowed 60 seconds to explore freely in the water after being released from one of four starting locations. The time taken for the mice to find the platform was recorded as the escape latency. If mice could not find the platform within 60 seconds, the escape latency was recorded as 60 seconds and the mice were trained to find the platform. After five consecutive days of the hidden platform experiment, the platform was removed, and the probe trial was conducted on the sixth day. The mouse was released from the northeast (NE) quadrant, and the swimming path, swimming time ratio and distance ratio in the SW quadrant were recorded within 60 seconds.

## Fecal Sample Collection and DNA Extraction

After the MWM test, fecal samples from each mouse were collected in sterile tubes and stored at  $-80^\circ\text{C}$  in a refrigerator. The total genomic DNA of the microbial community was extracted from these fecal samples according to the instructions, and the integrity of the extracted genomic DNA was detected by 1% agarose gel electrophoresis. The DNA concentration and purity were determined using NanoDrop2000 (Thermo Scientific, USA).

## PCR Amplification and Sequencing Library Construction

PCR amplifications were constructed using the primers ITS1F (CTTGGTCATTTAGAGGAAGTAA) and primers ITS2R (GCTGCGTTCTTCATCGATGC), which carries the barcode sequence and target the ITS2 rRNA genes. TaKaRa rTaq DNA Polymerase was employed for PCR amplification, with the reaction parameters set to  $95^\circ\text{C}$  for 3 minutes, followed by 27 cycles ( $95^\circ\text{C}$  for 30 seconds, annealing at  $55^\circ\text{C}$  for 30 seconds,  $72^\circ\text{C}$  for 45 seconds). A final extension was performed at  $72^\circ\text{C}$  for 10 minutes, and the samples were stored at  $4^\circ\text{C}$  (PCR instrument: ABI GeneAmp<sup>®</sup> 9700). PCR products were recovered using a 2% agarose gel, followed by product purification. The recovered products were detected and quantified using a Quantus<sup>™</sup> Fluorometer (Promega, USA). The NEXTFLEX<sup>™</sup> Rapid DNA-Seq Kit (Bioo Scientific, Austin, Texas, USA) was applied to build the library of the purified PCR products. Sequencing was performed using the PE300/PE250 platform of Illumina Company (Shanghai Majorbio Bio-pharm Technology Co.,Ltd).<sup>29</sup>

## ELISA Analysis

After MWM test, six mice in each group were euthanized with pentobarbital sodium (150 mg/kg). Hippocampus tissues were harvested and homogenized in ice-cold RIPA lysis buffer. The levels of A $\beta$ 40 and A $\beta$ 42 were measured using ELISA kit (PI310, Beyotime, China), with all specific steps conducted in strict accordance with the manufacturer's instructions.

## Immunofluorescence Staining

After MWM test, six mice in each group were anesthetized with pentobarbital (80 mg/kg) and perfused with 4% paraformaldehyde. The brains were dissected and fixed in 4% paraformaldehyde. Following sucrose dehydration and embedding, the brain tissues were sectioned coronally to a thickness of 6  $\mu$ m using a Microtome Cryostat (CM1900, Leica Corporation, Germany). The rabbit polyclonal antibody to  $\beta$ -amyloid (36–6900, Invitrogen, United States) was used as the primary antibodies. The corresponding secondary antibody was donkey anti-rabbit IgG Alexa Fluor 488 (ab150073, Abcam, United States). After washing and blocking, the  $\beta$ -amyloid antibody was added dropwise to the sections and incubated overnight at 4 °C. After washing, the sections were treated with the secondary antibodies. Finally, the sections were stained with Fluoroshield Mounting Medium with DAPI (ab104139, Abcam, United States) and examined under a confocal laser scanning microscope (SP8, Leica, United States). Identical exposure times and image settings were applied to each experiment. For each sample, the CA1 region of the hippocampus was selected as the target area, and three visual fields were randomly selected for detection as previously described.<sup>30</sup> The mean optical density of each image was calculated via Image J software (National Institutes of Health, MD, USA).

## Hematoxylin and Eosin Analysis

After MWM test, three mice in each group were anesthetized with pentobarbital (80 mg/kg) and perfused with 4% paraformaldehyde. The brains were dissected and fixed in 4% paraformaldehyde. Following sucrose dehydration and embedding, the brain tissues were sectioned by a Microtome Cryostat (CM1900, Leica Corporation, Germany). The sections were immersed in hematoxylin stain for 5 minutes. After washing, 1% hydrochloric acid alcohol differentiated for 2 seconds. After washing, PBS reblued for 5 minutes. After washing, sections were stained with eosin stain for 1–3 minutes, followed by dehydration sealing. The histopathological changes of the hippocampus were observed microscopically (Leica, United States) at 400 $\times$  magnification. For each sample, the CA1 and CA3 areas of the hippocampus were designated as the target area. These morphological observations were independently validated by two pathologists in a blinded manner to ensure consistency.

## Nissl Staining

After MWM test, six mice in each group were anesthetized with pentobarbital (80 mg/kg) and perfused with 4% paraformaldehyde. The brains were dissected and fixed in 4% paraformaldehyde. Following sucrose dehydration and embedding, the brain tissues were sectioned using a Microtome Cryostat (CM1900, Leica Corporation, Germany). The sections were fixed with 4% paraformaldehyde for 15 minutes, washed with PBS for 2 minutes, and stained with Nissl staining solution (Solarbio, G1430, China) for 7 minutes. After washing, the sections were placed in Nissl differentiation solution, rapidly dehydrated, and sealed with neutral gum. Neurons and Nissl bodies in the hippocampus were visualized with a biological microscope (Leica, United States) at 400 $\times$  magnification. For each sample, the CA1 and CA3 areas of the hippocampus were designated as the target area, and three non-repetitive visual fields were randomly selected for shooting.<sup>31,32</sup> The number of Nissl-positive neurons was quantified using Image J software (National Institutes of Health, MD, USA).

## Statistical Analysis

The statistical analysis was performed by SPSS 20.0 software (SPSS, Inc., Chicago, IL, United States). Correspondingly, the required graphs were generated by GraphPad Prism 8 software. All data were expressed as the mean  $\pm$  standard deviation. A two-way analysis of variance (ANOVA) with repeated measures was applied to dissect differences among groups in the hidden platform trial. One-way ANOVA with the Least Significant Difference (LSD) method was used to compare the variability among groups in other trials when the data were normally distributed or had homogenous variance. Otherwise, the non-parametric test would be used. Spearman's rank correlation test was used to perform correlation analyses. Statistical significance was defined as  $P < 0.05$ , while high statistical significance was defined as  $P < 0.01$ .



## Results

### Spatial Learning and Memory Ability of Mice in Each Group

On day 1, there were no significant differences in escape latency among the groups. The escape latencies of the WT, Ac and Pr groups decreased gradually on days 2–5 of the hidden platform experiment. However, the escape latency of the AD group always maintained a high level and was significantly higher than that of the WT group on days 2–5 ( $P < 0.01$ ). Notably, the escape latencies of the Ac and Pr groups on days 3–5 were remarkably lower than that of the AD group ( $P < 0.01$  or  $P < 0.05$ ), yet still higher than that of the WT group ( $P < 0.01$ ) (Figure 1A). No significant differences in swimming speed were found during the hidden platform trial (Figure 1B). In the probe trial, the swimming time ratio and the distance ratio in the SW quadrant for the AD group were drastically lower compared to the WT group ( $P < 0.01$ ). Conversely, the swimming time ratio and the distance ratio in the SW quadrant for the Ac and Pr groups were obviously higher than those observed in the AD group ( $P < 0.01$  or  $P < 0.05$ ) (Figure 1C and 1D). Analysis of swimming traces revealed distinct swimming strategies among the groups. The swimming traces of the AD group predominantly converged in the NE quadrant, while those of the WT, Ac and Pr groups primarily converged in the SW quadrant (Figure 1E).

### The Structure of Intestinal Fungal Community of Mice in Each Group

We utilized rarefaction curve analysis to assess the adequacy of the sequencing data. The results showed that the rarefaction curves for each group approached a plateau, indicating that the sequencing data had reached saturation and were therefore sufficient (Figure 2A). The Venn diagram illustrated that the four groups shared 100 operational taxonomic units (OTUs), with 139 OTUs unique to the WT group, 66 OTUs unique to the AD group, 102 OTUs unique to the Ac group, and 128 OTUs unique to the Pr group. In addition, the WT group shared 8 OTUs with the AD group, 21 OTUs with the Ac group, and 24 OTUs with the Pr group (Figure 2B). Subsequently, we evaluated the  $\beta$ -diversity of the fungal microbiota across the groups using the unweighted UniFrac algorithm. The principal coordinate analysis (PCoA) indicated significant differences among the groups ( $P < 0.05$ ), with samples from the WT and AD groups being clearly separated and exhibiting different species compositions (Figure 2C). The  $\alpha$ -diversity analysis revealed that the Sobs, Chao and Ace indices in the AD group were drastically lower than those in the WT group ( $P < 0.01$ ), while the Sobs, Chao, and Ace indices in the Ac and Pr groups were significantly higher than those in the AD group ( $P < 0.01$  or  $P < 0.05$ ) (Figure 2D-F).

### Taxonomic Changes of Intestinal Fungal Community of Mice in Each Group

We assessed the composition of the fungal microbiota across different taxonomic levels within each group. Sequencing analysis identified 4 phyla, 20 classes, 52 orders, 97 families, 148 genera and 247 species. The Circos diagram at the phylum level indicated that *Ascomycota* and *Basidiomycota* were the predominant phyla in all groups of mice. Specifically, *Ascomycota* was the principal phylum in the WT, Ac, and Pr groups, whereas both *Ascomycota* and *Basidiomycota* were predominant in the AD group (Figure 3A). At the genus level, the bar diagram illustrated that the five genera with the highest abundance were *Penicillium*, *Fusarium*, *Candida*, *Talaromyces*, and *Aspergillus*. Among these, the dominant genera in the WT, Ac and Pr groups were *Penicillium*, *Fusarium*, and *Talaromyces*, while in the AD group, *Penicillium* and *Candida* were the dominant genera (Figure 3B). Subsequently, we conducted a comparative analysis of the relative abundance of various fungal taxa across different taxonomic levels, including phylum, family, and genus. At the phylum level, the AD group exhibited an obviously higher abundance of *Ascomycota* and a significantly lower abundance of *Basidiomycota* compared to the WT group ( $P < 0.01$ ). In contrast, the Ac group showed a marked decrease in the abundance of *Ascomycota* compared to the AD group ( $P < 0.01$ ), while the abundance of *Basidiomycota* increased substantially in both the Ac and Pr groups ( $P < 0.01$ ) (Figure 3C and D). At the family level, the abundance of *Aspergilaceae* and *Trichocomaceae* was obviously higher in the AD group compared to the WT group ( $P < 0.01$ ). Compared with the AD group, the abundance of *Aspergilaceae* was drastically lower in the Ac and Pr groups, and the abundance of *Trichocomaceae* was markedly lower in the Ac group ( $P < 0.05$ ) (Figure 3E and F). At the genus level, compared with the WT group, the abundance of *Candida* and *unclassified-penicillium* in the AD group increased significantly ( $P < 0.01$ ). While the abundance of *Candida* and *unclassified-penicillium* in the Ac and Pr groups decreased dramatically compared to the AD group ( $P < 0.01$  or  $P < 0.05$ ) (Figure 3G and H).

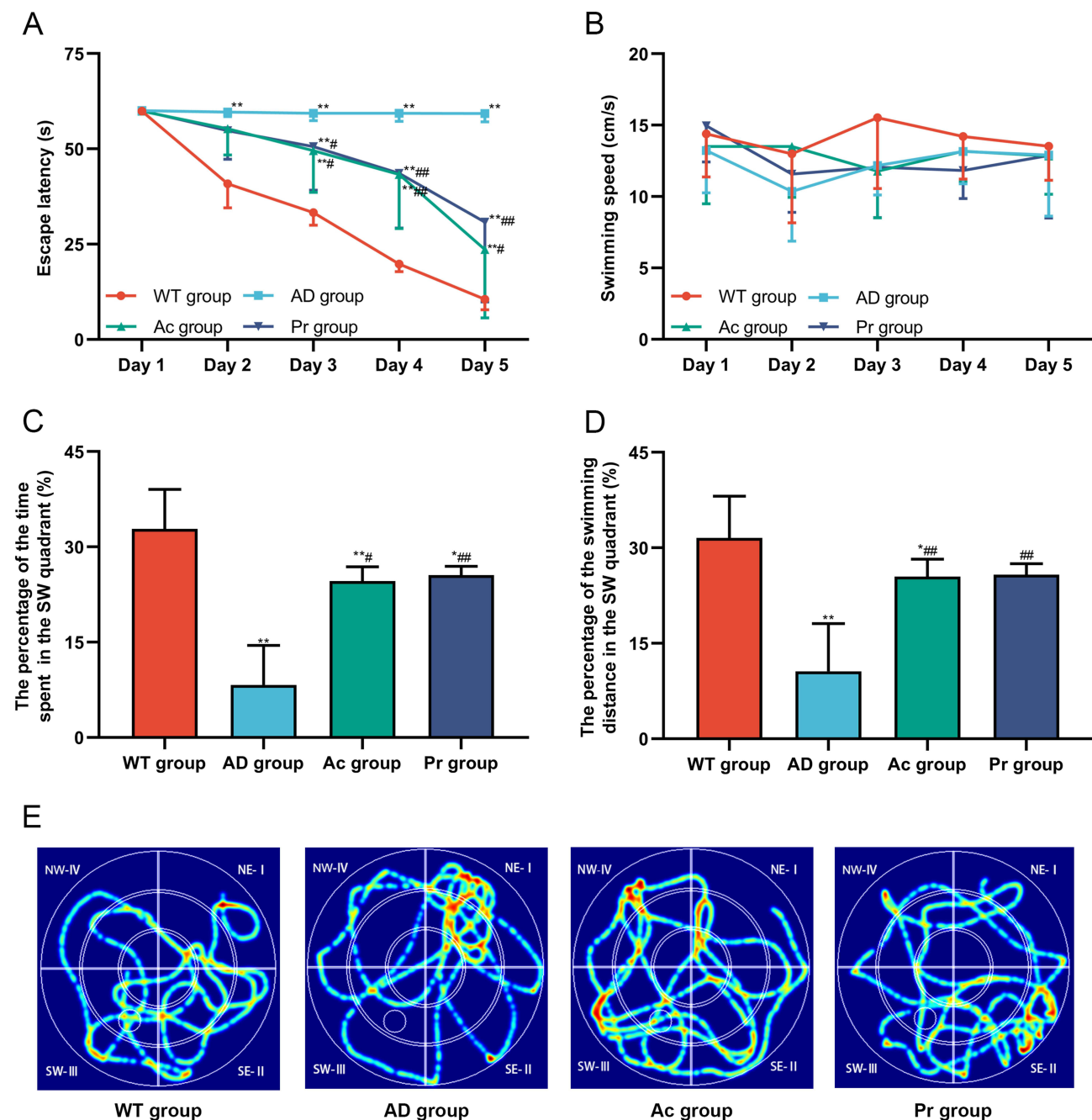


**Figure 1** Spatial learning and memory ability of mice in each group.

**Notes:** (A) The escape latency of each group in the hidden platform trial. (B) The swimming speed of each group in the hidden platform trial. (C) The swimming time ratio in the SW quadrant of each group in the probe trial. (D) The swimming distance ratio in the SW quadrant of each group in the probe trial. (E) The training traces of each group in the probe trial. Data were expressed as means  $\pm$  SEM ( $n = 10$ ), \* $P < 0.05$ , \*\* $P < 0.01$  versus the WT group; # $P < 0.05$ , ### $P < 0.01$  versus the AD group.

**Abbreviations:** SW, southwest; AD, Alzheimer's disease; WT, wild-type.

## Correlation Analysis Between Hippocampal A $\beta$ 40 and A $\beta$ 42 Levels and the Intestinal Fungal Community at the Phylum Level

The results of correlation heatmap analysis indicated that hippocampal levels of A $\beta$ 40 and A $\beta$ 42 were positively correlated with the abundance of *Ascomycota* (A $\beta$ 40,  $r = 0.68$ ,  $P < 0.001$ ; A $\beta$ 42,  $r = 0.74$ ,  $P < 0.001$ ). Conversely, these levels exhibited a negative correlation with the abundance of *Basidiomycota* (A $\beta$ 40,  $r = -0.44$ ,  $P < 0.05$ ; A $\beta$ 42,  $r = -0.50$ ,  $P < 0.05$ ) and *Mucoromycota* (A $\beta$ 40,  $r = -0.46$ ,  $P < 0.05$ ; A $\beta$ 42,  $r = -0.45$ ,  $P < 0.05$ ) (Figure 4A).

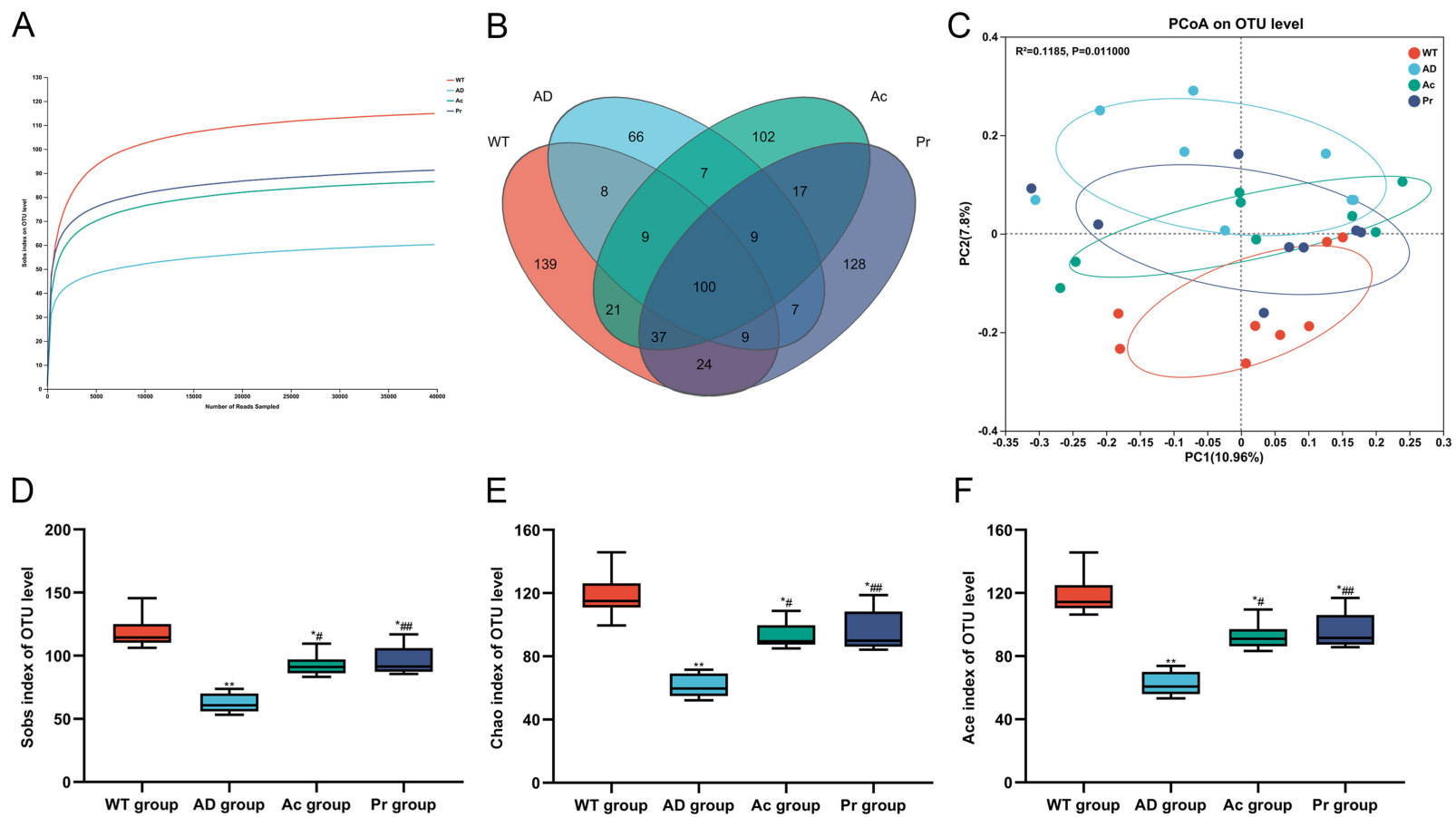


**Figure 2** The structure of intestinal fungal community of mice in each group.

**Notes:** (A) The rarefaction curves analysis in each group. (B) The venn diagram in each group. (C) PCoA analysis in each group. (D-F) The Sobs, Chao, Ace index in each group. Data were expressed as means  $\pm$  SEM ( $n = 8$ ), \* $P < 0.05$ , \*\* $P < 0.01$  versus the WT group; # $P < 0.05$ , ### $P < 0.01$  versus the AD group.

**Abbreviations:** AD, Alzheimer's disease; WT, wild-type; PCoA, principal coordinate analysis.

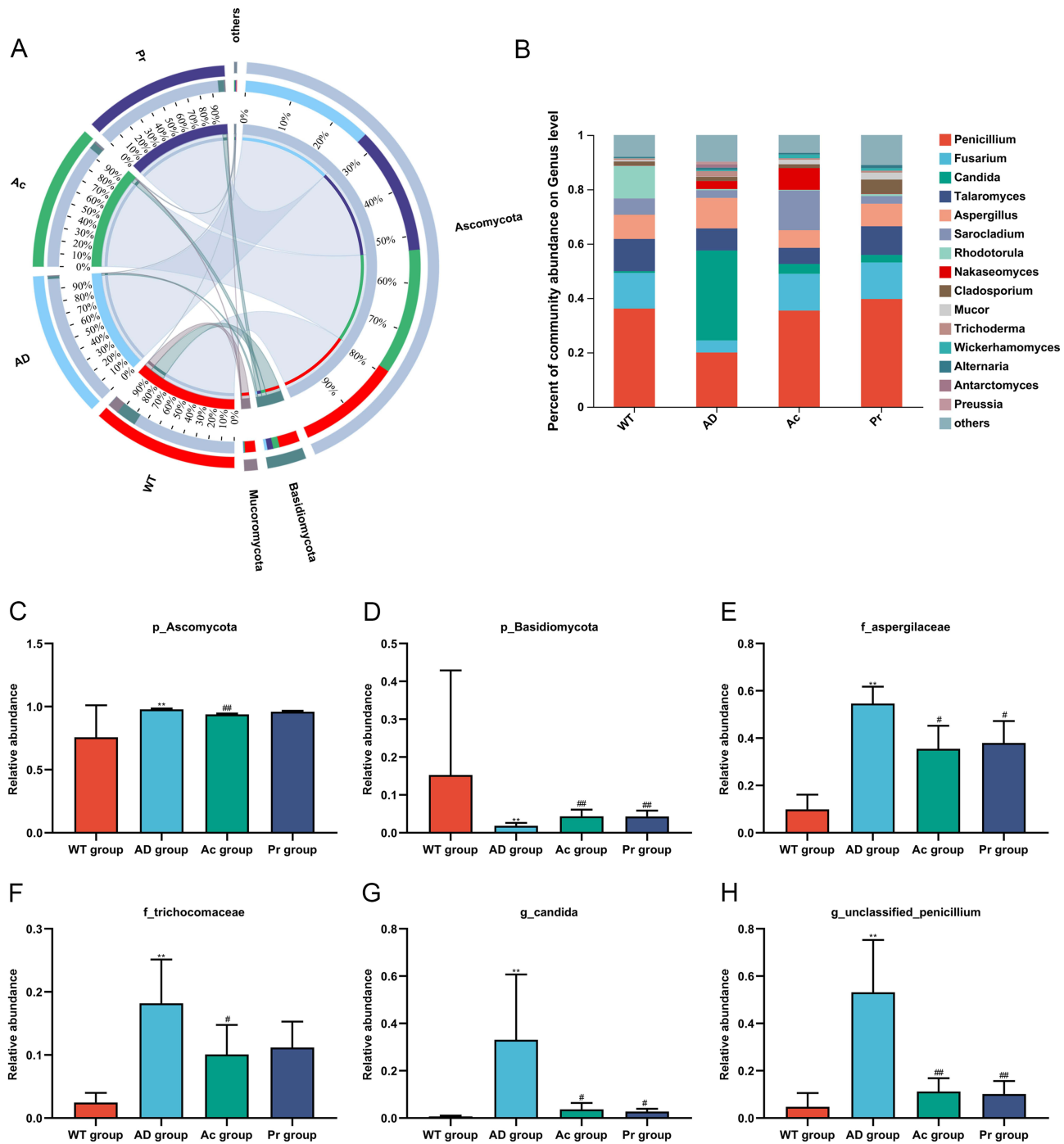


**Figure 3** Taxonomic changes of intestinal fungal community of mice in each group. **Notes:** (A) Circos diagram at the phylum level. (B) Bar diagram at the genus level. (C-D) Comparison of abundance at the phylum level in each group. (E-F) Comparison of abundance at the family level in each group. (G-H) Comparison of abundance at the genus level in each group. Data were expressed as means  $\pm$  SEM ( $n = 8$ ), \*\* $P < 0.01$  versus the WT group; # $P < 0.05$ , ### $P < 0.01$  versus the AD group. **Abbreviations:** AD, Alzheimer's disease; WT, wild-type.

# The Changes of A $\beta$ Deposition in the Brain of Mice in Each Group

IF staining analysis showed that numerous A $\beta$ -positive plaques were significantly aggregated in the hippocampus of mice in the AD group, whereas almost no A $\beta$  plaques were observed in the WT group. The deposition of A $\beta$  plaques was notably lower in the Ac and Pr groups compared to the AD group (Figure 4B). Compared with the WT group, the mean optical density of A $\beta$  plaques in the hippocampus of the AD group was significantly increased ( $P < 0.01$ ). Compared with

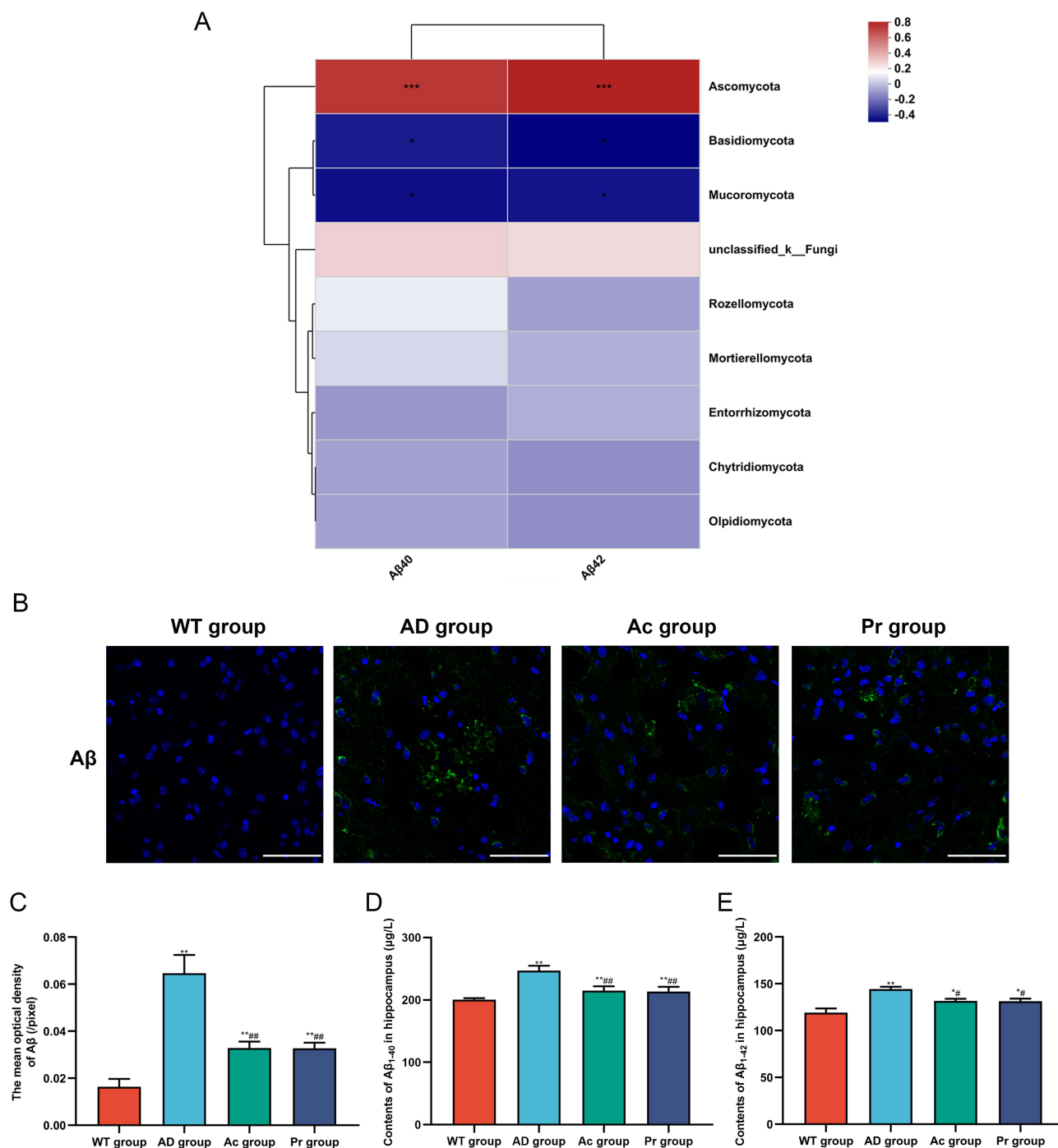


**Figure 4** Aβ level of mice in each group.

**Notes:** (A) Correlation analysis between the levels of Aβ<sub>40</sub> and Aβ<sub>42</sub> in hippocampus and intestinal fungal community at phylum level, \*indicates a  $P < 0.05$ , \*\*\*indicates a  $P < 0.001$ . (B) Representative images of IF staining of Aβ in each group. The scale bar is 50 μm. (C) The mean optical density of Aβ in each group. (D-E) The concentrations of Aβ<sub>40</sub> and Aβ<sub>42</sub> in each group. Data were expressed as means ± SEM ( $n = 6$ ), \* $P < 0.05$ , \*\* $P < 0.01$  versus the WT group; # $P < 0.05$ , ### $P < 0.01$  versus the AD group. **Abbreviations:** Aβ, β-amyloid; AD, Alzheimer's disease; WT, wild-type; IF, immunofluorescence.

the AD group, the mean optical density of Aβ plaques in the hippocampus of the Ac and Pr groups decreased dramatically ( $P < 0.01$ ), but it was still markedly higher than that of the WT group ( $P < 0.01$ ) (Figure 4C).

The concentrations of Aβ<sub>40</sub> and Aβ<sub>42</sub> in brain homogenate of mice in each group were detected by ELISA. The results indicated that the concentrations of Aβ<sub>40</sub> and Aβ<sub>42</sub> in the hippocampus of the AD group were obviously higher than those in the WT group ( $P < 0.01$ ). The concentrations of Aβ<sub>40</sub> and Aβ<sub>42</sub> in the hippocampus of the Ac and Pr



groups were significantly lower than those in the AD group ( $P < 0.01$  or  $P < 0.05$ ), but still significantly higher than those in the WT group ( $P < 0.01$  or  $P < 0.05$ ) (Figure 4D and E).

## Morphological Characteristics of Hippocampal Neurons of Mice in Each Group

In the WT group, neurons within the CA1 and CA3 regions of the hippocampus exhibited clear staining, were tightly arranged, and showed no significant reduction in number. The nuclei were round, and the nucleoli were distinct. Conversely, neurons in the AD group displayed disorganization, with poorly defined nuclei and evidence of nuclear consolidation. Subjectively, compared with the AD group, neurons in the Ac and Pr groups demonstrated more orderly arrangements, with better structural integrity and less nuclear condensation (Figure 5A). Furthermore, we used Nissl staining to evaluate neural state in the hippocampus of mice (Figure 5B). Nissl bodies were distributed in cell bodies and dendrites. The number of Nissl-positive neurons in the hippocampal CA1 and CA3 regions was significantly lower in the AD group than in the WT group. ( $P < 0.01$ ). Compared with the AD group, the number of Nissl-positive neurons in the Ac and Pr groups increased significantly ( $P < 0.01$  or  $P < 0.05$ ), yet it remained markedly lower than that in the WT group ( $P < 0.01$  or  $P < 0.05$ ) (Figure 5C and D).

## Discussion

The pathological aggregation of A $\beta$  represents a hallmark neuropathological feature of AD, which induces progressive neurodegeneration through multiple mechanisms, ultimately resulting in synaptic dysfunction and cognitive decline.<sup>33</sup> Increasing evidence indicates that dysregulation of the microbe-gut-brain axis is implicated in the pathogenesis of neurodegeneration in AD.<sup>34</sup> As a crucial component of the gut microbiome, intestinal fungi play a pivotal role in the progression of AD. Researches have demonstrated the occurrence of fungal microbiota dysbiosis in AD patients, which contributes to neuroinflammation and the accumulation of A $\beta$  in the brain.<sup>1,14</sup> Therefore, regulating the intestinal fungal community to reduce A $\beta$  plaque burden in the brain may represent a potential therapeutic strategy for ameliorating cognitive dysfunction in AD. In this study, we confirmed that acupuncture could effectively ameliorate cognitive impairment of APP/PS1 mice, concomitantly reducing A $\beta$  plaque burden in the hippocampus. In addition, acupuncture was found to improve the diversity of intestinal fungi and maintain the balance of the intestinal fungal community in APP/PS1 mice. These discoveries suggest that intestinal fungi may serve as a potential target for acupuncture in ameliorating cognitive dysfunction and brain amyloidosis in APP/PS1 mice.

In the behavioral test, our findings revealed no significant differences in swimming speeds among the various groups of mice, suggesting that their swimming abilities were equivalent. Consequently, any potential confounding effects of swimming ability on the experimental outcomes were effectively ruled out. Mice in the AD group exhibited poorer performance in the MWM test compared to the WT group, indicating that the cognitive ability of APP/PS1 mice was impaired, which aligns with the pathological characteristics of cognitive deficits observed in AD patients.<sup>35</sup> Both acupuncture and probiotics markedly improved the cognitive function of APP/PS1 mice, and their therapeutic effects were comparable, which was consistent with our previous study.<sup>24</sup>

The deposition of A $\beta$  in the hippocampus induces neuroinflammation and oxidative stress, which can cause neurodegenerative pathologies in AD.<sup>36</sup> Moreover, A $\beta$  is recognized as an upstream activator of pathological tau protein phosphorylation, which ultimately leads to neuronal death.<sup>37,38</sup> It has been reported that cognitive decline in AD patients is closely related to A $\beta$  deposition.<sup>39</sup> Therefore, inhibiting A $\beta$  aggregation or promoting its clearance in the brain is beneficial to alleviate nerve injury and delay the cognitive decline in AD. In this study, we identified numerous A $\beta$ -positive plaques accompanied by substantial neuronal damage in the hippocampus of APP/PS1 mice. Elevated levels of A $\beta$ 40 and A $\beta$ 42 were also detected via ELISA in the AD group. A $\beta$ 40 and A $\beta$ 42 peptides are generated through the proteolytic cleavage of amyloid precursor protein (APP) by  $\beta$ - and  $\gamma$ -secretases. These peptides can aggregate in the brain, forming senile plaques that contribute to neuronal damage.<sup>40</sup> Our research demonstrated that acupuncture significantly alleviated A $\beta$  plaque load and neuronal loss in the hippocampus of APP/PS1 mice. This finding corresponds with prior research showing that acupuncture has been proven to improve cognitive function by reducing A $\beta$  deposition and protecting neurons.<sup>41,42</sup>

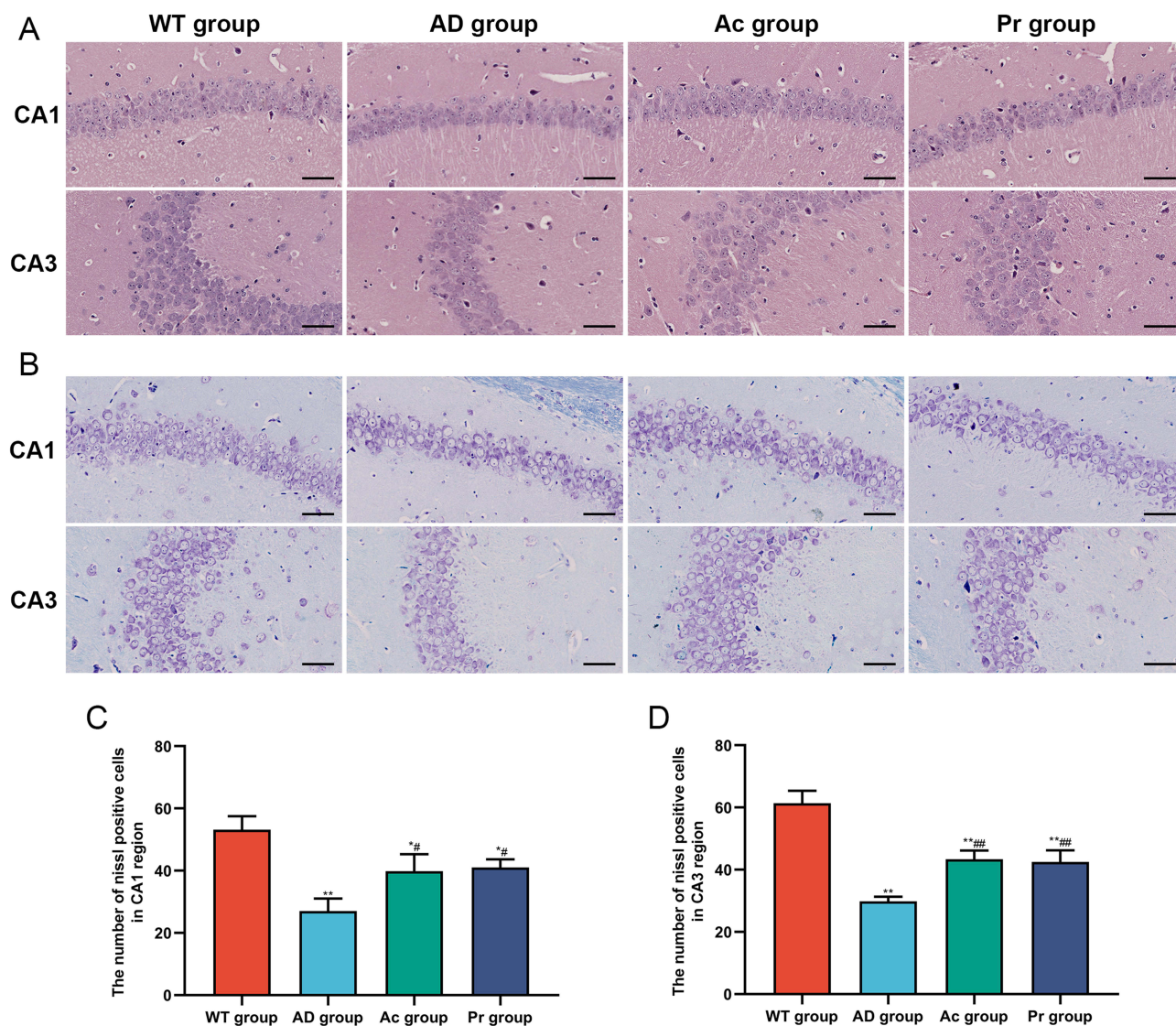


**Figure 5** HE and Nissl staining in CA1 and CA3 regions of hippocampus of mice in each group.

**Notes:** (A) Representative images of HE staining. The scale bar is 60  $\mu$ m. (B) Representative images of Nissl staining. The scale bar is 60  $\mu$ m. (C) The number of Nissl staining positive cells in the CA1. (D) The number of Nissl staining positive cells in the CA3. Data were expressed as means  $\pm$  SEM ( $n = 6$ ), \* $P < 0.05$ , \*\* $P < 0.01$  versus the WT group; # $P < 0.05$ , ### $P < 0.01$  versus the AD group.

**Abbreviations:** HE, hematoxylin and eosin; AD, Alzheimer's disease; WT, wild-type.

The formation of amyloid plaques is often associated with an imbalance in intestinal microbiota. The appearance of gut inflammation and microbial dysbiosis in AD model animals has been proved to precede the deposition of A $\beta$  in the brain.<sup>43</sup> Fecal transplants from healthy mice have demonstrated a reduction in A $\beta$  levels and Tau protein phosphorylation in the brains of AD model mice, leading to improved behavioral outcomes.<sup>44</sup> Although intestinal fungi represent only a minor component of the gut microbiome, their influence on the host organism is significant. Research indicates that the fungal microbiota is involved in the regulation of cognitive functions and behavior, playing a critical role in the pathogenesis of AD.<sup>12,14,45</sup> Leonardi et al<sup>46</sup> revealed that intestinal fungi can influence neuronal function through the brain-gut axis. Ye et al<sup>15</sup> identified dysbiosis of the fungal microbiota in APP/PS1 mice, which aligns with the findings of our study. Specifically, our results demonstrated that APP/PS1 mice exhibited a reduced  $\alpha$ -diversity index and significantly altered  $\beta$ -diversity compared to C57BL/6 mice. Consistent with these findings, prior research has reported that fungal diversity within the gut microbiota of adults decreases progressively with age.<sup>47</sup> In our study, acupuncture significantly enhanced the richness of the intestinal fungal communities in APP/PS1 mice, making the microbiota of

these animals more similar to that of healthy subjects. Furthermore, our analysis of community composition revealed substantial changes in the intestinal fungi of APP/PS1 mice across various taxonomic levels. The APP/PS1 mice treated with acupuncture showed a notable decrease in the abundance of *Ascomycota*, *Aspergilaceae*, *Trichomaceae*, *Candida*, and *unclassified-penicillium* and a simultaneous increase in *Basidiomycota*. Interestingly, Wang et al<sup>16</sup> reported a dramatic decrease in the abundance of *Ascomycota* and *Basidiomycota* phyla in A $\beta$ 1-42-injected AD rats. Another study indicated that the abundance of *unclassified-sordariomycetes* order was higher in the 3xTg-AD mice compared to the WT mice.<sup>48</sup> These findings differed from the fungal alterations we observed in APP/PS1 mice, potentially attributable to the intricate interplay of multiple factors that influence the gut microbiota. The composition of the intestinal fungal microbiome can vary among individuals with different backgrounds of AD and experimental animal models. Previous research has demonstrated that *Ascomycota* and *Basidiomycota* are dominant in the composition of fungal microorganisms, and the changes in their ratio often mean an imbalance in the fungal community, which is related to cognitive decline.<sup>14,49</sup> Studies have found that *Candida*, *Aspergilaceae* and *Trichomaceae* are dramatically enriched in the intestines of AD patients.<sup>1,50</sup> The proliferation of *Candida* may induce intestinal inflammation and impair the intestinal mucosal barrier. Once the intestinal barrier is compromised, *Candida* can translocate into the bloodstream and subsequently breach the blood-brain barrier, where it can form hyphae, activate microglia, and promote amyloid deposition.<sup>51–53</sup> *Mycotoxins* produced by *Aspergillus* can disrupt neuroimmune homeostasis and trigger neuroinflammation.<sup>54,55</sup> *Penicillium*, a member of the *Ascomycota* phylum, may disrupt the balance between intestinal fungi and bacteria, thereby increasing the risk of AD.<sup>56</sup> Collectively, our data implied that acupuncture may exert a therapeutic effect on AD by mitigating intestinal fungal dysbiosis. It is crucial to emphasize that, while probiotics also possess the capacity to regulate the intestinal fungal community, the specific fungal taxa influenced by acupuncture differ from those affected by probiotic intervention. In our study, probiotics were found to alter the abundance of *Basidiomycota*, *Aspergilaceae*, *Candida* and *unclassified-penicillium*, yet had no significant impact on the abundance of *Ascomycota* and *Trichomaceae*. This discrepancy may be attributed to the distinct action mechanisms of acupuncture and probiotics. Furthermore, the fungal species modulated by probiotics in our study differed from those reported by Ye et al,<sup>15</sup> potentially owing to the use of different probiotic strains.

We confirmed the relationship between intestinal fungi and the levels of A $\beta$ 40 and A $\beta$ 42 in the hippocampus of APP/PS1 mice using Spearman analysis, which revealed a strong correlation between A $\beta$  deposition and the abundance of *Ascomycota*, *Basidiomycota* and *Mucoromycota*. In conclusion, these findings suggest that intestinal fungi dysbiosis may contribute to the accumulation of A $\beta$  in the brain and exacerbate the pathology of AD. The beneficial effects of acupuncture and probiotics on hippocampal A $\beta$  deposition and cognitive function in APP/PS1 mice might be mediated by enhancing intestinal fungal diversity and modulating the composition of the fungal community. *Ascomycota* and *Basidiomycota* could serve as promising targets for acupuncture to reduce A $\beta$  deposition.

Most notably, in our experimental design, the WT, AD, and Pr groups underwent the same mouse bag fixation procedures as the Ac group. This rigorous control measure ensures that any alterations observed in intestinal fungal composition and A $\beta$  deposition in APP/PS1 mice can be attributed to the specific effects of the acupuncture intervention, independent of potential confounding factors associated with the restraint procedure. Such methodological considerations strengthen the validity of our conclusions regarding the specific therapeutic effects of acupuncture to a certain extent. Additionally, this restraint protocol was established and refined through our previous investigations,<sup>23,30,57</sup> representing a well-optimized methodology that ensures optimal comfort for the animals during acupuncture treatment and greatly reduces stress responses.

Our research still has certain limitations. Although preliminary evidence supports the notion that acupuncture can ameliorate A $\beta$  deposition and cognitive impairment by balancing intestinal fungi, we have not yet been able to conduct reverse validation of these findings. Future studies should incorporate a treatment group in which acupuncture is administered concurrently with antifungal agents, such as fluconazole, to eliminate intestinal fungi. This approach aims to further substantiate the hypothesis that intestinal fungi serve as a potential target for the neuroprotective effects of acupuncture.



## Conclusion

Our study reconfirmed that acupuncture could improve the cognitive impairment of APP/PS1 mice, reduce the A $\beta$  plaque burden in the brain, and protect neurons. We identified for the first time that acupuncture could increase the diversity of intestinal fungi and modulate the composition of the intestinal fungal community in APP/PS1 mice. This modulation is characterized by a decrease in the abundance of *Ascomycota*, *Aspergilaceae*, *Trichocomaceae*, *Candida*, and *unclassified-penicillium*, alongside an increase in *Basidiomycota*. Additionally, we speculated that the beneficial effects of acupuncture on A $\beta$  deposition and cognitive function in APP/PS1 mice might be achieved by regulating the intestinal fungal community.

## Ethics Approval and Consent to Participate

All animal experiments were conducted in accordance with the protocol approved by Beijing University of Chinese Medicine, Beijing, China (ID: bucm-4-2021102701-4032).

## Acknowledgments

Thanks for the support of the online platform of Majorbio Cloud Platform.

## Funding

This research was supported by the National Natural Science Foundation of China (No. 82004482, 82274654), the China Academy of Chinese Medical Sciences Fund for Excellent Young Scholars (No. ZZ14-YQ-012), and the Yong Elite Scientists Sponsorship Program by BAST (No. BYESS2023339).

## Disclosure

The authors report no conflicts of interest in this work.

## References

1. Phuna ZX, Madhavan P. A closer look at the mycobiome in Alzheimer's disease: fungal species, pathogenesis and transmission. *Eur. J. Neurosci.* 2022;55(5):1291–1321. doi:10.1111/ejn.15599
2. Walsh DM, Selkoe DJ. Amyloid  $\beta$ -protein and beyond: the path forward in Alzheimer's disease. *Curr Opin Neurobiol.* 2020;61:116–124. doi:10.1016/j.conb.2020.02.003
3. Chen C, Liao J, Xia Y, et al. Gut microbiota regulate Alzheimer's disease pathologies and cognitive disorders via PUFA-associated neuroinflammation. *Gut.* 2022;71(11):2233–2252. doi:10.1136/gutjnl-2021-326269
4. Kesika P, Suganthy N, Sivamaruthi BS, Chaiyasut C. Role of gut-brain axis, gut microbial composition, and probiotic intervention in Alzheimer's disease. *Life Sci.* 2021;264:118627. doi:10.1016/j.lfs.2020.118627
5. Seo DO, Holtzman DM. Current understanding of the Alzheimer's disease-associated microbiome and therapeutic strategies. *Exp mol Med.* 2024;56(1):86–94. doi:10.1038/s12276-023-01146-2
6. Hamad I, Ranque S, Azhar EI, et al. Culturomics and amplicon-based metagenomic approaches for the study of fungal population in human gut microbiota. *Sci Rep.* 2017;7(1):16788. doi:10.1038/s41598-017-17132-4
7. Ferreira AL, Choi J, Ryou J, et al. Gut microbiome composition may be an indicator of preclinical Alzheimer's disease. *Sci Transl Med.* 2023;15(700):eabo2984. doi:10.1126/scitranslmed.abo2984
8. Hadrich I, Turki M, Chaari I, et al. Gut mycobiome and neuropsychiatric disorders: insights and therapeutic potential. *Front Cell Neurosci.* 2024;18:1495224. doi:10.3389/fncel.2024.1495224
9. Huseyin CE, O'Toole PW, Cotter PD, Scanlan PD. Forgotten fungi-the gut mycobiome in human health and disease. *FEMS Microbiol Rev.* 2017;41(4):479–511. doi:10.1093/femsre/fuw047
10. D'Argenio V, Veneruso I, Gong C, Cecarini V, Bonfili L, Eleuteri AM. Gut microbiome and mycobiome alterations in an in vivo model of Alzheimer's disease. *Genes (Basel).* 2022;13(9):1564. doi:10.3390/genes13091564
11. Hashimoto K, Anderson R, Bambah-Mukku D, Carta I, Autry AE. Emerging role of the host microbiome in neuropsychiatric disorders: overview and future directions. *mol Psychiatry.* 2023;28(1):1–13. doi:10.1038/s41380-022-01915-x
12. Ling Z, Zhu M, Liu X, et al. Fecal fungal dysbiosis in Chinese patients with Alzheimer's Disease. *Front Cell Dev Biol.* 2020;8:631460. doi:10.3389/fcell.2020.631460
13. Cirstea MS, Sundvick K, Golz E, et al. The gut mycobiome in Parkinson's disease. *J Parkinsons Dis.* 2021;11(1):153–158. doi:10.3233/JPD-202237
14. Nagpal R, Neth BJ, Wang S, Mishra SP, Craft S, Yadav H. Gut mycobiome and its interaction with diet, gut bacteria and Alzheimer's disease markers in subjects with mild cognitive impairment: a pilot study. *EBioMedicine.* 2020;59:102950. doi:10.1016/j.ebiom.2020.102950
15. Ye T, Yuan S, Kong Y, et al. Effect of probiotic fungi against cognitive impairment in mice via regulation of the fungal microbiota-gut-brain axis. *J Agric Food Chem.* 2022;70(29):9026–9038. doi:10.1021/acs.jafc.2c03142
16. Wang L, Lu Y, Liu J, et al. Gegen qinlian tablets delay Alzheimer's disease progression via inhibiting glial neuroinflammation and remodeling gut microbiota homeostasis. *Phytomedicine.* 2024;128:155394. doi:10.1016/j.phymed.2024.155394

17. Ding N, Jiang J, Xu A, Tang Y, Li Z. Manual acupuncture regulates behavior and cerebral blood flow in the samp8 mouse model of Alzheimer's disease. *Front Neurosci.* 2019;13:37. doi:10.3389/fnins.2019.00037
18. Cao J, Tang Y, Li Y, Gao K, Shi X, Li Z. Behavioral changes and hippocampus glucose metabolism in APP/PS1 transgenic mice via electro-acupuncture at governor vessel acupoints. *Front Aging Neurosci.* 2017;9:5. doi:10.3389/fnagi.2017.00005
19. Li Y, Jiang J, Tang Q, et al. Microglia TREM2: a potential role in the mechanism of action of electroacupuncture in an Alzheimer's disease animal model. *Neural Plast.* 2020;2020:8867547. doi:10.1155/2020/8867547
20. Sun RQ, Wang ZD, Zhao J, et al. Improvement of electroacupuncture on APP/PS1 transgenic mice in behavioral probably due to reducing deposition of  $\text{A}\beta$  in hippocampus. *Anat Rec (Hoboken).* 2021;304(11):2521–2530. doi:10.1002/ar.24737
21. Yang Q, Zhu S, Xu J, et al. Effect of the electro-acupuncture on senile plaques and its formation in APP+/PS1+ double transgenic mice. *Genes Dis.* 2019;6(3):282–289. doi:10.1016/j.gendis.2018.06.002
22. Li G, Zhang X, Cheng H, et al. Acupuncture improves cognitive deficits and increases neuron density of the hippocampus in middle-aged SAMP8 mice. *Acupunct Med.* 2012;30(4):339–345. doi:10.1136/acupmed-2012-010180
23. Hao X, Ding N, Zhang Y, et al. Benign regulation of the gut microbiota: the possible mechanism through which the beneficial effects of manual acupuncture on cognitive ability and intestinal mucosal barrier function occur in APP/PS1 mice. *Front Neurosci.* 2022;16:960026. doi:10.3389/fnins.2022.960026
24. Zhang Y, Ding N, Hao X, et al. Manual acupuncture benignly regulates blood-brain barrier disruption and reduces lipopolysaccharide loading and systemic inflammation, possibly by adjusting the gut microbiota. *Front Aging Neurosci.* 2022;14:1018371. doi:10.3389/fnagi.2022.1018371
25. Jiang J, Liu G, Shi S, Li Y, Li Z. Effects of manual acupuncture combined with donepezil in a mouse model of Alzheimer's disease. *Acupunct Med.* 2019;37(1):64–71. doi:10.1136/acupmed-2016-011310
26. Liu W, Zhuo P, Li L, et al. Activation of brain glucose metabolism ameliorating cognitive impairment in APP/PS1 transgenic mice by electroacupuncture. *Free Radic Biol Med.* 2017;112:174–190. doi:10.1016/j.freeradbiomed.2017.07.024
27. Ni Y, Yang X, Zheng L, et al. Lactobacillus and bifidobacterium improves physiological function and cognitive ability in aged mice by the regulation of gut microbiota. *mol Nutr Food Res.* 2019;63(22):e1900603. doi:10.1002/mnfr.201900603
28. Tian H, Ding N, Guo M, et al. Analysis of learning and memory ability in an Alzheimer's disease mouse model using the Morris water maze. *J Vis Exp.* 2019; 152. doi:10.3791/60055
29. Han C, Shi C, Liu L, et al. Majorbio Cloud 2024: update single-cell and multiomics workflows. *Imeta.* 2024;3(4):e217. doi:10.1002/imt2.217
30. Ding N, Jiang J, Tian H, Wang S, Li Z. Benign regulation of the astrocytic phospholipase A2-arachidonic acid pathway: the underlying mechanism of the beneficial effects of manual acupuncture on CBF. *Front Neurosci.* 2019;13:1354. doi:10.3389/fnins.2019.01354
31. Sun Y, Xu L, Zheng D, et al. A potent phosphodiesterase Keap1-Nrf2 protein-protein interaction inhibitor as the efficient treatment of Alzheimer's disease. *Redox Biol.* 2023;64:102793. doi:10.1016/j.redox.2023.102793
32. Long QH, Wu YG, He LL, et al. Suan-zao-ren decoction ameliorates synaptic plasticity through inhibition of the  $\text{A}\beta$  deposition and JAK2/STAT3 signaling pathway in AD model of APP/PS1 transgenic mice. *Chin Med.* 2021;16(1):14. doi:10.1186/s13020-021-00425-2
33. Chen Y, Qi Z, Qiao B, Lv Z, Hao Y, Li H. Oxymatrine can attenuate pathological deficits of Alzheimer's disease mice through regulation of neuroinflammation. *J Neuroimmunol.* 2019;334:576978. doi:10.1016/j.jneuroim.2019.576978
34. Tremlett H, Bauer KC, Appel-Cresswell S, Finlay BB, Waubant E. The gut microbiome in human neurological disease: a review. *Ann Neurol.* 2017;81(3):369–382. doi:10.1002/ana.24901
35. Jaroudi W, Garami J, Garrido S, Hornberger M, Keri S, Moustafa AA. Factors underlying cognitive decline in old age and Alzheimer's disease: the role of the hippocampus. *Rev Neurosci.* 2017;28(7):705–714. doi:10.1515/revneuro-2016-0086
36. Liu Y, Zhang H, Peng A, et al. PEG-PEI/siROCK2 inhibits  $\text{A}\beta$ 42-induced microglial inflammation via NLRP3/caspase 1 pathway. *Neuroreport.* 2022;33(1):26–32. doi:10.1097/WNR.0000000000001752
37. Lane CA, Hardy J, Schott JM. Alzheimer's disease. *Eur J Neurol.* 2018;25(1):59–70. doi:10.1111/ene.13439
38. Liao D, Miller EC, Teravskis PJ. Tau acts as a mediator for Alzheimer's disease-related synaptic deficits. *Eur J Neurosci.* 2014;39(7):1202–1213. doi:10.1111/ejn.12504
39. Willem M, Fändrich M. A molecular view of human amyloid- $\beta$  folds. *Science.* 2022;375:6577:147–148.
40. Sciacaluga M, Megaro A, Bellomo G, et al. An unbalanced synaptic transmission: cause or consequence of the amyloid oligomers neurotoxicity? *Int J Mol Sci.* 2021;22(11):5991. doi:10.3390/ijms22115991
41. Zhang T, Guan B, Tan S, et al. Bushen huoxue acupuncture inhibits NLRP1 inflammasome-mediated neuronal pyroptosis in SAMP8 mouse model of Alzheimer's disease. *Neuropsychiatr Dis Treat.* 2021;17:339–346. doi:10.2147/NDT.S279304
42. Xu M, Lin R, Wen H, et al. Electroacupuncture enhances the functional connectivity of limbic system to neocortex in the 5xFAD mouse model of Alzheimer's disease. *Neuroscience.* 2024;544:28–38. doi:10.1016/j.neuroscience.2024.02.025
43. Honarpisheh P, Reynolds CR, Blasco Conesa MP, et al. Dysregulated gut homeostasis observed prior to the accumulation of the brain amyloid- $\beta$  in Tg2576 mice. *Int J Mol Sci.* 2020;21(5):1711. doi:10.3390/ijms21051711
44. Sun J, Xu J, Ling Y, et al. Fecal microbiota transplantation alleviated Alzheimer's disease-like pathogenesis in APP/PS1 transgenic mice. *Transl Psychiatry.* 2019;9(1):189. doi:10.1038/s41398-019-0525-3
45. Alonso R, Pisa D, Aguado B, Carrasco L. Identification of fungal species in brain tissue from Alzheimer's disease by next-generation sequencing. *J Alzheimers Dis.* 2017;58(1):55–67. doi:10.3233/JAD-170058
46. Leonardi I, Gao IH, Lin WY, et al. Mucosal fungi promote gut barrier function and social behavior via Type 17 immunity. *Cell.* 2022;185(5):831–846.e14. doi:10.1016/j.cell.2022.01.017
47. Sender R, Fuchs S, Milo R. Revised estimates for the number of human and bacteria cells in the body. *PLoS Biol.* 2016;14(8):e1002533. doi:10.1371/journal.pbio.1002533
48. Cecarini V, Gogoi O, Bonfili L, et al. Modulation of gut microbiota and neuroprotective effect of a yeast-enriched beer. *Nutrients.* 2022;14(12):2380. doi:10.3390/nu14122380
49. Coker OO, Nakatsu G, Dai RZ, et al. Enteric fungal microbiota dysbiosis and ecological alterations in colorectal cancer. *Gut.* 2019;68(4):654–662. doi:10.1136/gutjnl-2018-317178
50. Gonzalez-Lara MF, Ostrosky-Zeichner L. Invasive Candidiasis. *Semin Respir Crit Care Med.* 2020;41(1):3–12. doi:10.1055/s-0040-1701215



51. Wu Y, Du S, Johnson JL, et al. Microglia and amyloid precursor protein coordinate control of transient *Candida* cerebritis with memory deficits. *Nat Commun.* **2019**;10(1):58. doi:10.1038/s41467-018-07991-4
52. A S, Tm F, Cm S, et al. *Candida albicans*-induced epithelial damage mediates translocation through intestinal barriers. *mBio.* **2018**;9(3).
53. Kim MS, Kim Y, Choi H, et al. Transfer of a healthy microbiota reduces amyloid and tau pathology in an Alzheimer's disease animal model. *Gut.* **2020**;69(2):283–294. doi:10.1136/gutjnl-2018-317431
54. Ladd TB, Johnson JA, Mumaw CL, et al. *Aspergillus versicolor* Inhalation Triggers Neuroimmune, Glial, and Neuropeptide Transcriptional Changes. *ASN Neuro.* **2021**;13:17590914211019886. doi:10.1177/17590914211019886
55. Park S, Lee JY, You S, Song G, Lim W. Neurotoxic effects of aflatoxin B1 on human astrocytes in vitro and on glial cell development in zebrafish in vivo. *J Hazard Mater.* **2020**;386:121639. doi:10.1016/j.jhazmat.2019.121639
56. Shen B, Cao Z, Wu Y, et al. Purlisin, a toxin-like defensin derived from clinical pathogenic fungus *Purpureocillium lilacinum* with both antimicrobial and potassium channel inhibitory activities. *FASEB J.* **2020**;34(11):15093–15107. doi:10.1096/fj.202000029RR
57. Jiang J, Liu H, Wang Z, et al. Electroacupuncture could balance the gut microbiota and improve the learning and memory abilities of Alzheimer's disease animal model. *PLoS One.* **2021**;16(11):e0259530. doi:10.1371/journal.pone.0259530

## Neuropsychiatric Disease and Treatment

### Publish your work in this journal

Neuropsychiatric Disease and Treatment is an international, peer-reviewed journal of clinical therapeutics and pharmacology focusing on concise rapid reporting of clinical or pre-clinical studies on a range of neuropsychiatric and neurological disorders. This journal is indexed on PubMed Central, the 'PsycINFO' database and CAS, and is the official journal of The International Neuropsychiatric Association (INA). The manuscript management system is completely online and includes a very quick and fair peer-review system, which is all easy to use. Visit <http://www.dovepress.com/testimonials.php> to read real quotes from published authors.

Submit your manuscript here: <https://www.dovepress.com/neuropsychiatric-disease-and-treatment-journal>

**Dovepress**  
Taylor & Francis Group